Multisided patches
with B-spline boundaries

Núria Pla, Marc Vigo, Josep Cotrina

Research Report LSI-04-33-R

Computer Graphics Section — Dept. LSI.
Universitat Politècnica de Catalunya

Multisided patches

N. Pla-Garcia, M. Vigo-Anglada, J. Cotrina-Navau

2004

Abstract

We present a method to construct a patch of parametric surface of degree $k+1$ that fills a n-sided hole, with n bigger than 2, and whose boundary coincides with a B-Spline, thus, the resulting patch can be easily connected with given B-Spline surfaces with fixed continuity conditions.

The method is inspired on a generic approach to construct free form surfaces, which gives a family of practical schemes to design surfaces from an arbitrary given mesh, using the differentiable manifold theory.

The input is a star shaped mesh which describes a generic n-hole and a surface in a neighborhood of the hole. The main advantages of the method are the following: arbitrary order k continuity conditions can be imposed; the involved hole can have an arbitrary number of sides and arbitrary shape (convex or not); the simplicity of the construction process gives an easy and flexible method; and finally, the surface near the boundary is a B-Spline with piecewise uniform knot sequences and whose control points are vertices of the given mesh; both knot sequences and control points are easily computed. Implementation details to evaluate a surface point are given, showing that the de Boor algorithm can be exploited for efficiency.

Keywords:Computer Aided Geometric Design, B-Splines, N-Sided patches, continuity

1 Introduction

The representation of free form surfaces is a very important topic in Computer Graphics. Generally, the surfaces are defined by an assembly of rectangular patches. However in some cases, rectangular patches leave some n-sided holes. Many methods have been proposed for constructing non-four-sided patches (see [Sab83, HK84, LD89, Var91, EC97, ZA97, SZSS98], among others). Overviews of these methods can be found in [Var87] and [Mal98].

The problem of the n-patch construction is treated from different perspectives in the existing literature. In some cases, a given set of patches, of a specific class, makes a n-sided hole that has to be filled with certain degree of continuity. In other cases, a method for constructing arbitrary n-sided patches is proposed, and properties of the resulting patch are studied. The approach presented in this paper belongs to the second type of methods.

In any case, the methods for constructing n-sided patches can be classified into recursive subdivision, surface splitting, data blending and control point schemes.

The method presented in this paper can be classified among the data blending schemes. It is a fully automatic method for easily obtaining an order k continuous surface from a control mesh that surrounds a hole with n sides, the parameters $n > 2$ and $k \geq 0$ being arbitrary integers. It is a barycentric method and the resulting surface will approximate the input mesh both topologically and geometrically. The shape of the patch depends on a scalar value f, called the aperture factor. This value f can vary between some limits and determines the influence of the control points on the central part of the patch. Besides, the construction allows adding extra layers of interior control points to shape the central part of the patch without loosing the smooth connection in the boundaries. Both the aperture factor and the extra layers shape the central part of the n-sided patch, in a similar way than the "midpoint" in the approach of Varady [Var91]. Furthermore, the boundary sides of the patch coincide with a tensor product B-Spline whose control points are vertices of the input mesh.

Our approach can be understood as a realization of the generic scheme presented in [CPV02]. In previous articles we presented two different realizations of this generic scheme. In the first realization, [CP00a], the input mesh has to be planar, and this fact is exploited to easily construct the surface. However, in [CP00a] the shape of the charts is not related to the faces of the mesh (even when projected): all charts are rectangular, while the faces can be free shaped. In the second realization, [CP00b], the input mesh has a totally arbitrary topology. In this case, the mesh is split into rectangular submeshes and planar star-shaped submeshes. The shape of the charts in this second realization does depend on the shape of the input faces, once preprocessed. Both realizations could have been used for the type of meshes treated in this article, since it is a planar mesh that could be transformed into a star-shaped sub-mesh plus few regular submeshes. However, the approach we propose here takes advantage of the specific topology of the mesh, giving place to a global construction (the mesh does not have to be split) and using chart shapes similar to the one of the corresponding input faces. By imposing the shape and chart distribution, we obtain a surface with good properties, such that it has B-Spline boundaries. Note that although the input mesh has a specific topology, we solve a classical problem in CAGD.

The rest of the paper is organized as follows: Section 2 presents the problem definition and an overview of the process followed to define the n-sided patches; in Section 3 the preprocess applied to the input mesh is detailed; Section 4 presents the different steps followed to define the surface of the patch and properties of the resulting surface are obtained; Section 5 shows that each boundary of a n-sided patch coincides with a B-spline. Besides, in this section we give an example showing how to compute knot sequences and control points of the B-Spline representation. Section 6 gives an algorithm to evaluate any surface point given its parametric coordinates, and the procedures involved in point evaluation are further detailed. In Section 7 several examples of n-sided patches are shown, and some questions concerning our proposal are discussed;

finally, in Section 8 conclusions and some future work are presented. Notation details can be found in Appendixes A and B.

2 Problem definition and overview of the proposed solution

The method proposed in this paper constructs a k continuous parametric surface, with k an arbitrary input value, from a given mesh, $M \subset R^3$, which describes a regular n-sided hole. The input mesh could be understood as a sketch of a surface with a n-sided hole. Thus, the problem we dealt with can be seen as a construction of a n-sided patch given an input mesh with a particular configuration. The resulting n-sided patch approximates both topologically and geometrically the given mesh.

The problem we are facing is similar to the one solved in [Pra97], but in our case we have a different configuration of the input mesh, and there is not an extraordinary central point (which in the case of [Pra97] gives additional information about the geometrical behavior of the surface near the center of the hole).

Our proposal takes special care of the patch behavior near its boundaries, in order that it can be smoothly connected with other patches of a classical kind. In fact, in a neighborhood of each side of the resulting n-sided patch the surface coincides with a tensor product B-Spline.

2.1 The control net

The input mesh M is composed of s regular mesh layers around a central n-sided face. (By *regular mesh* we mean a vertex lattice, that is, a mesh whose faces have four sides and whose non-boundary vertices have degree four). The exact topology of the input mesh is next described.

The central face of the mesh is defined by n vertices of degree four, $n \geq 3$. Two consecutive degree-four vertices describe a side of the central face. Each side of the central face has, besides the two degree-four vertices, $r_m - 1$ vertices of degree three, for $m = 0, \ldots, n-1$.

The mesh M is defined as the union of s regular layers surrounding the n-sided hole (see Figure 1(a)). Notice that M is composed of $2n$ regular sub-meshes. There is a regular sub-mesh for each side, composed of $(r_m+1)\times(s+1)$ vertices, and a regular sub-mesh with $(s+1) \times (s+1)$ vertices associated to each four-degree vertex of the hole.

2.2 Overview of the proposed solution

Here a brief overview of the method proposed to construct the surface from a mesh is presented. The construction steps basically follow the idea presented in [CPV02]. The main difference is that in the method presented here the mesh

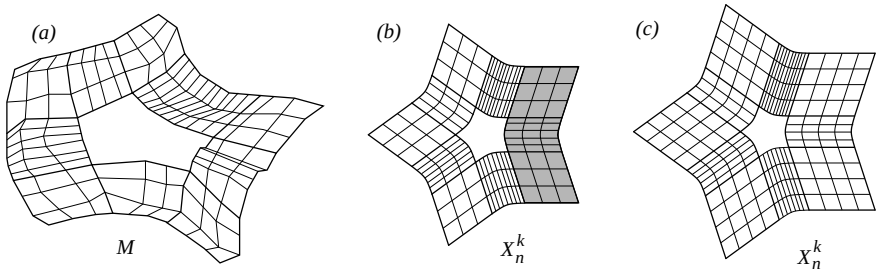

Figure 1: (a) Mesh defining a $n = 5$ sided hole. (b) The corresponding configuration of a 5-sided regular patch in parametric space for the case k is even. (c) The parametric space for the same case and odd k. The shaded part in (b) corresponds to one of the sides X_m.

defining the parameter space is not always homeomorphic to the input mesh M. In fact, when k is odd it is homeomorphic to the dual of M.

Let M be a mesh as the one described in the previous subsection. Figure 1(a) shows a 5-sided hole surrounded by 3 layers of regular mesh. The construction process is divided in the following steps, described in more detail in further sections.

1. First, we construct an auxiliary planar mesh, called *k-continuous regular n-hole configuration* and notated by X_n^k. This mesh defines the parameter space of the resulting surface. The exact configuration of X_n^k only depends on the degree continuity k and on the topology of M (i.e., it depends on n, r_m and s values). It admits some degree of freedom since a parameter f, called the aperture value, can be varied between some limits.

2. A set of charts is defined. Depending on the parity of the k-value, each chart is associated to a vertex or to a face of the mesh. The charts either have rectangular shape or are the drag of a spline curve along a straight line. The set of charts covers the parametric space, in particular it fills the hole defined by the regular mesh.

3. A basis function and a control point are defined for each chart. Basis functions define a unity partition over the mesh, and control points are the vertices of the original mesh.

4. The surface is built as the barycentric map defined in the parameter space, using the control points and the basis functions.

3 The mesh and its pre-process

The n-sided patch is defined from a control mesh M made of s layers of vertices surrounding a polygonal hole with n sides. Let r_m be as defined in Section 2.1.

The layers are distributed forming rectangular faces in the following way: the interior vertices have degree 4; the outer boundary vertices have degree 3, except for n that have degree 2; and the inner boundary vertices have degree 3, except for the n that have degree 4 (the ones that determine the n-sided hole). Figure 1(a) represents an example of a 5-sided mesh with $s = 3$ and $r_0 = 5, r_1 = 10, r_2 = 4, r_3 = 6, r_4 = 3$.

The parameters s and k, that is, the number of layers and the surface continuity are related (but not restrictive). For a large continuity order, the number of regular layers must increase so that the *irregular* part of the n-patch (that is, the part of the surface filling the hole) is isolated from the boundary.

A *k-continuous regular n-hole configuration* is defined as a mesh $X_n^k \subset \mathbb{R}^2$ with the topology described previously (that means, with a n-sided central face and surrounded by s layers of regular vertices) such that its vertices are distributed "piecewise equidistant".

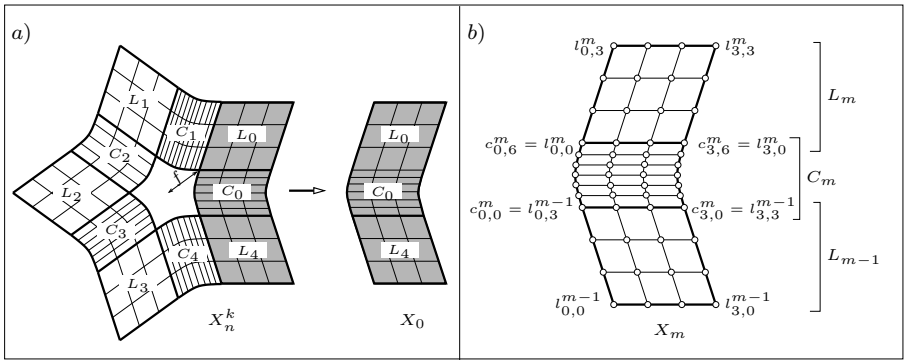

Figure 2: (a) Configuration of a n-patch mesh; one of its sides is separated. (b) Notations for a side X_m of a 5-sided patch with $s = 3$, $r_m = 6$.

Mesh vertices of X_n^k are defined making use of the symmetry of the construction: the whole star-shaped mesh is divided into n sub-meshes, called *sides* of the star and denoted by $X_0, \ldots X_{n-1}$ (see Figure 2(b)). These sides are not disjoint subsets, since X_m and X_{m+1} share vertices and faces. Since this is a circular division, from now on operations involving indices of the sides are considered to work modulo n. It is also useful to consider the representation of X_m in M, denoted by M_m.

We distinguish three parts in X_m: the sub-meshes L_m, L_{m-1} and C_m. Sub-meshes L_m and L_{m-1} are composed of $(s+1)\times(s+1)$ vertices, and sub-mesh C_m is composed of $(s+1)\times(r_m+1)$ vertices. All these three sub-meshes are regular (see Figure 2 for these notations). Notice that two consecutive sub-meshes X_m and X_{m+1} share some vertices of the mesh, thus these vertices have different labels associated. Furthermore, labels for vertices in L_m sub-meshes depend on the side m it is considered.

The geometric placement of vertices of X_n^k is represented in Figure 2: vertex

coordinates depend on the C^k curve μ defining the left and right boundaries of X_0, and the distance of each vertex to the center is determined by the aperture factor f. For the interested reader, the exact placement of coordinate vertices can be found in Appendix A.

The way a k-continuous regular n-hole configuration X_n^k is attached to any input mesh M depends on the parity of k in the following way: when k is even, X_n^k is the planar regular n-sided patch with the same topology than M. When k is odd, X_n^k is the dual graph of the mesh M (if neither the central face nor the outer unbounded face are considered); this is accomplished by considering a planar regular n-sided patch just being described but taking $s(X_n^k) = s + 1$ layers and $r_m(X_n^k) = r_m - 1, \forall m$, divisions of each side. In this way, for k even each vertex $v \in X_n^k$ has its image vertex $V \in M$, and in the odd case, each face in X_n^k has its corresponding vertex in M. This difference is made to ensure B-splines surfaces in the boundaries of the patch, for any k value. Figure 1(b) shows the configuration of the 5-sided regular patch built from the mesh M in Figure 1(a) for the case k is even, and Figure 1(c) shows the configuration for the same input mesh when k is odd.

4 The C^k patch

To construct the n-sided patch we use the k-continuous regular n-hole configuration as parameter space. The construction process makes use of the symmetry and the regularity of the construction.

First, let us define a bijective continuous map F that transforms the side X_0 into a geometrically more simple shape in $\mathbb{R}^2$ (a rectangular mesh), denoted by E_0 (see Figure 3). This map allows us not only to work in an auxiliary simpler parametric space, which simplifies both the definition process and the implementation, but also to better understand the relationship between our spline scheme and B-splines. The exact definition of F can be found in Appendix B.

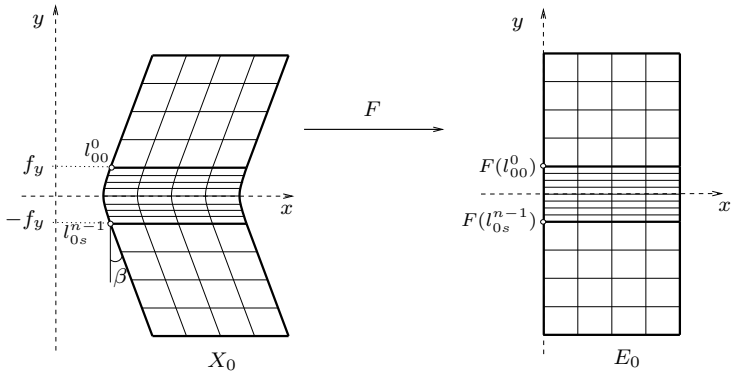

Figure 3: Mapping from X_0 to E_0.

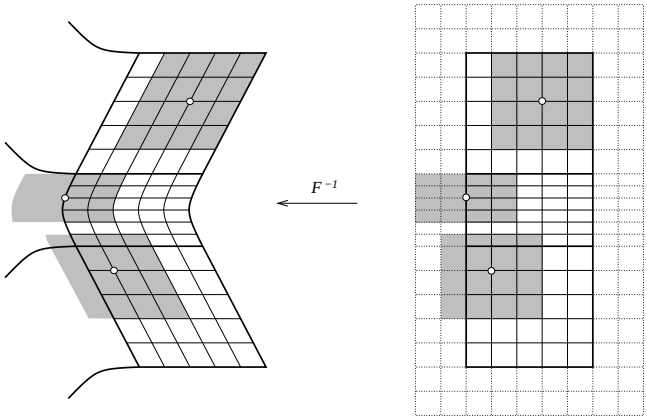

Figure 4: Charts definition process for the case they are centered on vertices ($k = 2, s = 5, r_m = 6$). Three different cases are represented.

4.1 The parameter space

We use X_n^k as parameter space with the manifold structure defined in this section. Thus, our proposal follows the generic scheme described in [CPV02]. The manifold structure is obtained from a set of charts and a set of transition functions. The precise definition of the charts and transition functions is one of the aspects that gives generality to the scheme proposed in [CPV02]. Therefore, it has to be detailed for the specific realization we are developing.

The set of charts we define satisfies the following properties: First, charts are geometrically simple subsets of $\mathbb{R}^2$, which is an important property since we use them as support for the basis functions. Second, each point inside X_n^k belongs to a minimum number of charts, which grants the simplicity of the construction as well as ensuring the smoothness of the resulting surface (this is best explained in next section). And third, charts near the boundary of the patch coincide with the ones that would be obtained for a B-spline with piecewise uniform knot distribution (this last property will be formalized in Section 5).

Depending on the parity of k we will define a chart for each vertex, when k is even, and a chart for each face of X_n^k (except for the n-sided hole face), when k is odd. To simplify the exposition we only consider the sub-mesh X_0, and we define the charts that are associated to the vertices. The charts for the rest of sides are defined symmetrically.

To define the charts we work in the space of E_0. Let $h = \lfloor k/2 \rfloor + 1$. First, h rectangular mesh layers are added to the four boundaries of E_0, giving place to the extended mesh E_0^+ (see Figure 4). These auxiliary layers are built according to the spacing between vertices of the mesh E_0 (see Figure 4). From now on, vertices of E_0^+ are notated as e_{ij}.

Sets z_{ij}^m are defined as the rectangles in E_0^+ that cover $(k+2) \times (k+2)$ mesh layers. There exists a z_{ij}^m set centered either on each vertex $e_{ij} \in E_0$ when k is

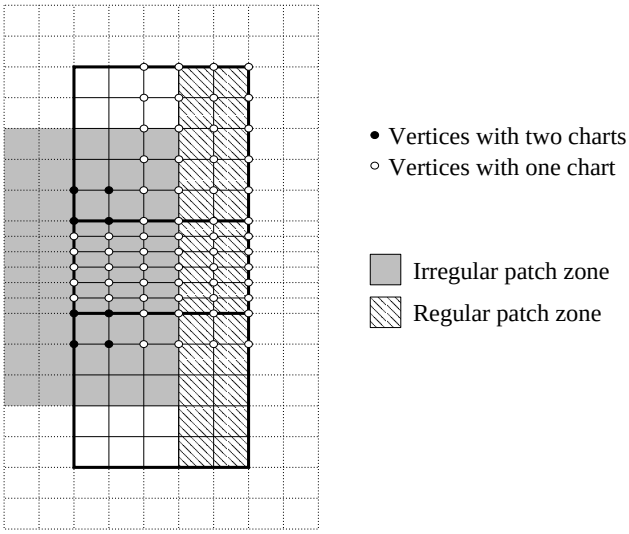

Figure 5: Vertices of a side E_m for which charts are to be considered are marked ($k = 2, s = 5, r_m = 6$), distinguishing between vertices with one chart associated and vertices with two charts associated. The regular patch zone Z_R and the irregular central part are also represented.

even, or on each face $f_{ij} \in E_0$ when k is odd. Notice that the extra layers are necessary in order that there exists a z_{ij} set for every vertex or for every face of E_0.

Then, charts $\mathcal{C}_{ij}^m$ for $i = 0, \ldots, s$ and $j = 0, \ldots, 2s + r_m$ are defined as $F^{-1}(z_{ij}^m)$.

Note that charts in X_n^k have a relatively simple shape, since they are a sweep of a curve along a straight segment. Figure 4 shows three different examples of charts.

According to this construction, a chart is defined for every element (i.e. vertex or face) of X_0. Since consecutive sides X_i and X_{i+1} have elements in common, if the definition above was used for the rest of sides, some elements of the regular n-sided patch would have two charts attached. In order to obtain a B-spline surface near the boundaries of the patch, duplicity of charts have to be avoided. In particular, for each side X_m, the following charts have to be discarded (see Figure 5):

$$\text{charts } \mathcal{C}_{ij}^m \text{ such that } j \geq s + r_m + h \text{ and } i < h \quad \text{, and} \tag{1}$$

$$\text{charts } \mathcal{C}_{ij}^m \text{ such that } j < s - h. \tag{2}$$

In this way, only some elements of X_m that are close to the hole of the n-sided patch have two charts associated (black vertices in Figure 5).

This definition associates a vertex or face of X_n^k to each chart, depending on the parity of k, and therefore each chart has a vertex of the original mesh M

associated. Remark, however, that some of these mesh vertices will have two (different) charts associated to it.

According to [CPV02], a family of transition functions is constructed to define the overlapping between the charts, but in the actual situation all the charts are defined in the regular n-sided patch, so the overlapping between charts is yet defined. Thus we define the transition functions as the identity map in $\mathbb{R}^2$. Thanks to this fact, in this case the continuity of the resulting surface is not restricted by the transition functions.

4.2 Surface generation

Once the parameter space with a manifold structure is defined, next step is to construct the surface, that is, the desired n-sided patch. We define a basis function associated to each chart, in fact, with support in the chart. We also define a control point associated to each chart. Then we use a barycentric scheme to construct the surface.

The map F simplifies the definition of a basis function for each chart. Recall that each chart $\mathcal{C}$ is the anti-image of a rectangular zone z_{ij}^m in E_m^+. Then, we define a tensor product B-spline basis function on this rectangle, denoted by $N_{\mathcal{C}}^k$, using as knot sequences the coordinates x and y, respectively, of the vertices in E_m^+.

Recall that while the majority of elements have a unique chart associated, some of them have two (see Section 4.1). Using a barycentric scheme would cause these elements to have double influence on the shape of the surface. Although in principle this is not a theoretical problem, in practice one expects all the control points to shape the surface in an homogeneous way. To avoid this, we define a normalizing factor $w_{\mathcal{C}}$ associated to each chart $\mathcal{C}$. For double association charts, $w_{\mathcal{C}} = 1/2$, and for the rest of charts $w_{\mathcal{C}} = 1$.

Since the overlapping of the charts does not follow exactly the overlapping that arise in a tensor product B-spline scheme (in the irregular part of the patch), we can not ensure that these functions determine a partition of the unity, so it is necessary to normalize them.

Therefore we define the basis functions as

$$\varphi_{\mathcal{C}}^k = \frac{w_{\mathcal{C}} N_{\mathcal{C}}^k}{\sum_{\mathcal{A} \in CS} w_{\mathcal{A}} N_{\mathcal{A}}^k}$$

where CS is the set of charts associated to elements in X_n^k.

As pointed out in Section 4.1, each chart is associated to a vertex or face of X_n^k. Since there is a one-to-one correspondence between elements of X_n^k and vertices of the control mesh M, a single vertex $P_{\mathcal{C}}$ of the mesh M is associated to each chart. This vertex $P_{\mathcal{C}}$ is taken as the control point associated to he chart $\mathcal{C}$.

Finally, the surface $S : X_n^k \subset \mathbb{R}^2 \to \mathbb{R}^3$ is defined as follows. Each chart $\mathcal{C}$ is associated to a control point $P_{\mathcal{C}}$ and to a basis function $\varphi_{\mathcal{C}}^k$, thus we can

compute the image of a parameter point u as

$$S(u) = \sum_{u \in \mathcal{C}} P_{\mathcal{C}}\, \varphi^k_{\mathcal{C}}(u).$$

Since this construction follows the scheme defined in [CPV02], we can ensure that the above surface has the following properties:

1. k-differentiability.
2. Affine invariance.
3. Local and global containment in the convex hull of the control mesh.

The computation of the manifold X^k_n, which is the most expensive step, only depends on the topology of the mesh and on the parameters f and k. Therefore, it can be performed only once for a given patch, even if the position of the control points is modified.

The shape of the resulting surface also depends on the aperture factor, since the size of central face depends on this value. Thus, if f is very large the number of charts covering the central part of the patch is too small, and thus an almost flat zone is produced. In the worst case, there can exist a region in the parametric space not covered by any chart. The aperture factor f must be bounded to avoid these undesirable effects.

Notice that in a usual tensor product surface each parametric point is covered by $(k+2)\times(k+2)$ charts. This is the minimum number of charts that we require for a 4-sided regular patch. A geometric reasoning shows that, in the general case, an analogous condition can be imposed if $2f\cos(\pi/n) < \lfloor k/2+1 \rfloor$ (this result is obtained by noticing that the most conflictive point is the center of X^k_n). In this way, we obtain a patch of a sufficient degree that allows a smooth enough free-form surface.

5 B-spline boundaries

We have defined a n-sided patch as an independent patch, but in practical situations this patch must be smoothly connected to existing surfaces. The advantage of our proposal resides in the fact that the boundaries of the n-patch coincide with B-splines, as the following theorem announces. Thus, the conditions for connecting a n-sided patch with a given B-spline rectangular patch are analogous to the ones obtained to connect two classical B-Spline patches.

Theorem 1. *If $s > k$ then the surface in a neighborhood of the boundary of the n-sided patch coincides with a B-Spline defined by some control points of M_m and knot distribution given by the vertex coordinates of E^+_m.*

Being more precise, given a side m, the regular part of the patch corresponds to a region Z_R in parametric space that covers a vertical stripe of $s-k-1$ mesh layers (see Figure 5). That is, the regular patch zone of a side m is the image $S(F^{-1}(Z_R))$ of the rectangle $Z_R \in E_m$) with extreme vertices $e_{0,k+1}$ and $e_{2s+m_k,s}$.

Recall that $s(X_n^k)$ is equal to s in the even case, and to $s+1$ in the odd case.

Proof. The proof for the Theorem is based on the proof of Theorem 1 in [CP00a], which states that any tensor product B-spline scheme can be obtained applying the generic scheme which is also the one used in the present paper. The construction of [CP00a] for a regular mesh and the restriction of the proposed method to Z_R are the same. We can ensure this because of the following facts:

1. Charts implied in the definition of $S(F^{-1}(Z_R))$ are not associated to elements with duplicate charts.

2. Since $s > k$, charts with non-empty intersection with Z_R are either charts associated to non-discarded vertices of E_m, or discarded charts associated to vertices in E_{m-1} whose definition coincides if side m is considered.

Thus, the definition for charts and control points for the portion of the surface we are considering is the same than the one for the B-spline case. □

Let us see an example. Figure 6 left shows an input mesh with parameters $n = 5, s = 4$ i $r_m = 2, \forall m$ (i.e. a 5-sided hole composed of 5 layers of points and 2 points in the central part of all sides). We choose $k = 2$ in this example. The points that determine the surface shape near the first boundary are the ones such that their attached charts cover the regular part Z_R. Since k is even, each chart is attached to a point of the input mesh. Charts cover a 4×4 rectangles in parametric space, thus points attached to these charts are the ones of the three rightmost columns of E_0 (emphasized in Figure 6 right). Therefore, the definition of the n-sided patch in this region coincides with a B-Spline whose control points are the ones of the three vertical columns near the side boundary of the input mesh (big points in Figure 6 left). The vertical knot sequence of the B-Spline is

$$(0, \delta, 2\delta, 3\delta, 4\delta, 5\delta, 6\delta, 6\delta+\gamma, 6\delta+2\gamma, 6\delta+3\gamma,$$
$$7\delta+3\gamma, 8\delta+3\gamma, 9\delta+3\gamma, 10\delta+3\gamma, 11\delta+3\gamma, 12\delta+3\gamma)$$

where δ and γ are the vertical distances between knots (see Appendix A). Horizontal knots are uniformly distributed, since points of E_0^+ are equally separated horizontally.

Notice that if the input mesh has the same number of points on each side (i.e. $r_0 = r_1 = r_2 = \ldots = r_n$), we obtain a totally uniform vertical knot distribution by imposing $\delta = \gamma$. This is equivalent to choosing the aperture factor to be

$$f = r_m cos(\pi/n)$$

6 Implementation

In this section we detail how to compute a point on the surface given its parametric coordinates $p = (x, y)$. The image point $S(p)$ is evaluated summing up

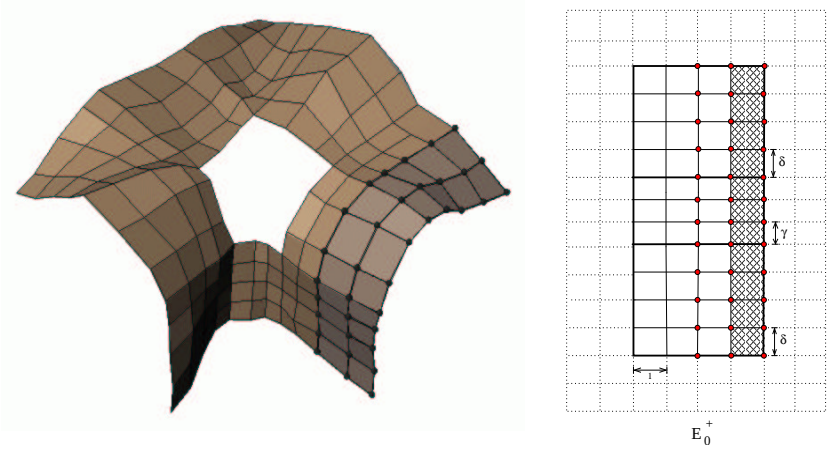

Figure 6: *Left*, mesh defining a 5-sided hole where the control points that define one of the B-Spline boundaries have been marked. *Right*, corresponding lattice points in the parametric space E_0. The shaded region is the regular part Z_R.

the terms of each chart $\mathcal{C}$ such that $p \in \mathcal{C}$, and then normalizing the result. The sum of basis functions is performed for each side M_m, traversing the charts associated to the mesh vertices in the spaces E_m. This results in the following algorithm, which given a point $p \in X_n^k$ computes its image point $S(p)$:

$(Sx, Sy, Sz, D) := (0, 0, 0, 0)$
per m **en** $[0..n-1]$ **fer**
  $p := Rotate(p, -2 * m * \pi/n)$
  $q := F(p)$
  $AddChartsOfSide(m, q, Sx, Sy, Sz, D)$
fper
$S(p) := (Sx/D, Sy/D, Sz/D)$

The rotation followed with the map F projects the point p from X_n^k to the parameter space of E_m^+. The core of the algorithm above is the procedure *AddChartsOfSide*, which actualizes the sum for the charts of a side m (the three coordinate components Sx, Sy, Sz and the sum of base functions D, used to normalize the result). These two processes are detailed in the next two subsections.

6.1 Computing F

The map $F(q)$ is implemented distinguishing three cases, corresponding to the three parts of $\tilde{\mu}(q)$: if q lies in the upper or lower part, then a single linear map is needed; otherwise, function μ intervenes in the computation. Notice that although in principle this computation depends on the parameter k, since μ is defined as a piecewise polynomial C^k curve smoothly connecting two segments,

in practice one could only consider the implementation for the maximum order of continuity admitted.

Let $q = (x, y)$ and let $l_{00}^m = (f_x, f_y)$. Then, if y is greater than f_y or smaller than $-f_y$, a simple linear transformation is needed. Otherwise, that is, if the point lies on the horizontal stripe corresponding to sub-mesh C_m, the mapping is given by the sweep of curve μ along a vertical segment.

Suppose that μ is parameterized in terms of y/f_y. Since the vertical spacing between consecutive vertices C_m is uniform, the parameter values t_i such that $\mu(t_i) = c_{ij}$ are also equally spaced.

Thus, we only need to identify the curve $\mu(t)$, or, more concretely, since the parameter value t coincides with y/f_y, the problem reduces to defining the horizontal term of the curve, $\mu_x(t)$. The definition for curve μ given in Appendix 1 gives

(5) $\mu_x(1) = \mu_x(-1) = f_x$

(6) $\mu_x{}'(1) = \tan(-\beta)$, $\mu_x(-1) = \tan(\beta)$

(7) $\mu_x^{(i)}(1) = \mu_x^{(i)}(-1) = 0$, $i = 2, \ldots, k$

where $\beta = \pi/2 - \alpha$. In fact, there is not a unique way to define this curve. In the actual implementation, we choose μ_x to be a polynomial. Thus, taking into account that the result has to be symmetric with respect to the x axis, the odd degree coefficients of the polynomial must be zero:

$$\mu_x(t) = a_{2k}t^{2k} + a_{2k-2}t^{2k-2} + \ldots + a_2t^2 + a_0$$

Imposing conditions above to this definition, a linear system of equations is obtained. Once solved, the $a_{2k} \ldots a_0$ coefficients are obtained. For example, for $k = 1$, we obtain a parabola,

$$\mu_x(t) = \frac{f_y \tan(\beta)}{2}(-t^2 + 1) + f_x$$

or for $k = 3$,

$$\mu_x(t) = \frac{f_y \tan(\beta)}{16}(-t^6 + 5t^4 - 15t^2 + 11) + f_x$$

Notice that this results in a quite simple function, and that although it has degree $2k$, it can be lowered to the half with a simple variable change $w = t^2$.

6.2 Adding charts

Procedure *AddChartsOfSide* actually computes which charts do affect a parametric point, once projected to E_m^+. In the main algorithm a traversal for all the sides m is done, and since elements of consecutive sides are shared, we have to avoid visiting twice shared vertices that have a single chart associated (see Section 4.1). Thus, for each side charts associated to vertices or faces fulfilling conditions (1) and (2) in Section 4.1 must not be taken into account.

For simplicity, we work in the spaces E_m^+, where the meshes and charts have rectangular shapes. This regular configuration can be exploited to use the usual algorithms developed for the tensor product B-Spline patches, as well as to perform bounding-box inclusion tests for improving the efficiency.

In particular, for the surface evaluation the de Boor algorithm for evaluating NURBS [Far02] can be used in the following way: (1) A fourth term, with unitary value, is added to the control points. This fourth coordinate is used in order that the de Boor algorithm also computes the sum term D (see algorithm above); (2) setting to zero all four coordinates of control points corresponding to discarded charts; and (3), the fourth coordinate is set to $1/2$ for all control points that have two charts associated, according to the definition of the surface given in Section 4.2. Notice that the de Boor algorithm must be applied not only to points in the standard parameter space for the NURBS case, but also to points belonging to an extension of E_m (see Figure 5).

In summary, the point evaluation essentially requires at most n mappings between the parametric spaces X_n^k and E_m plus n evaluations of an order $k+1$ B-spline rectangular patch with $(s+1) \times (2s + r_m + 1)$ four-dimensional control points. Since these extended control points are fixed, they can be pre-computed and stored so that multiple point evaluations are efficiently computed.

Notice also that one can improve the efficiency by pre-computing and storing the knot sequences. Besides, the horizontal knot sequence (the one corresponding to direction x) is common to all the E_m spaces, since horizontal knots are uniformly spaced and the number of knots is the same for all the sides. On the other hand, the vertical knot sequences (the y knot sequences) depend on the number of divisions of the side, r_m. Nevertheless, if all the sides have the same number of divisions, as seen in the example of Section 5, not only the vertical knot sequence is unique, but also, by choosing the appropriate aperture factor, the vertical spacing between all vertices in E_m can be forced to be the unit, so that a uniform B-spline scheme is obtained.

As we see, although the theoretical development of the multi-sided patch is quite complex, the method for point evaluation is rather simple, since efficient known algorithms for B-spline patches can be applied, and a strong usage of the symmetry can be exploited.

7 Results and discussions

Snapshots in Figures 7 to 11 show surfaces obtained by applying the method presented in this article from n-sided control meshes. In Figure 7, a 3-sided symmetric mesh is represented, and resulting surfaces computed by applying our method are shown. The different cases represented correspond to patches with continuity of order $k = 0, 1$ and 2.

Surfaces in Figure 8 are two C^2 patches, the left one is 5-sided and the right one is 6-sided that demonstrate the ability of the method for defining arbitrary n-sided patches from simple wire meshes. In the 6-sided patch, different zones of the patch have been represented in alternating colors in order to better appreci-

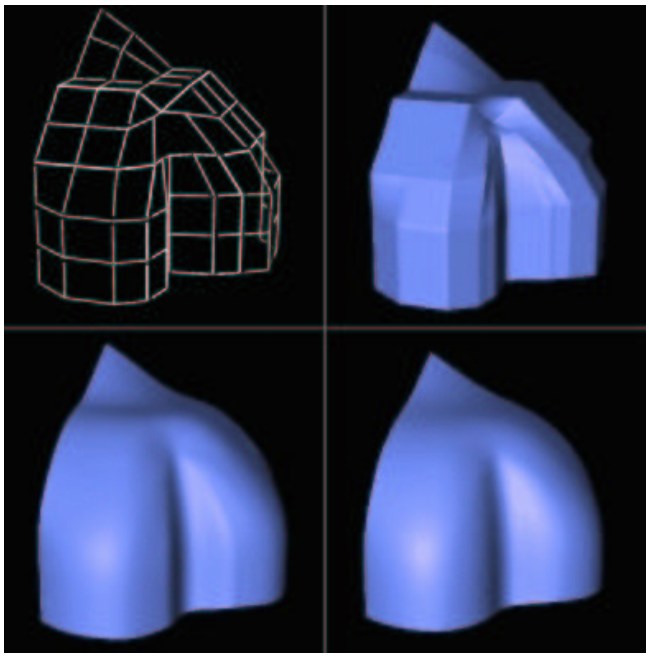

Figure 7: *Top left to bottom right:* Mesh defining a 3-sided hole, and surfaces of order 0, 1 and 2.

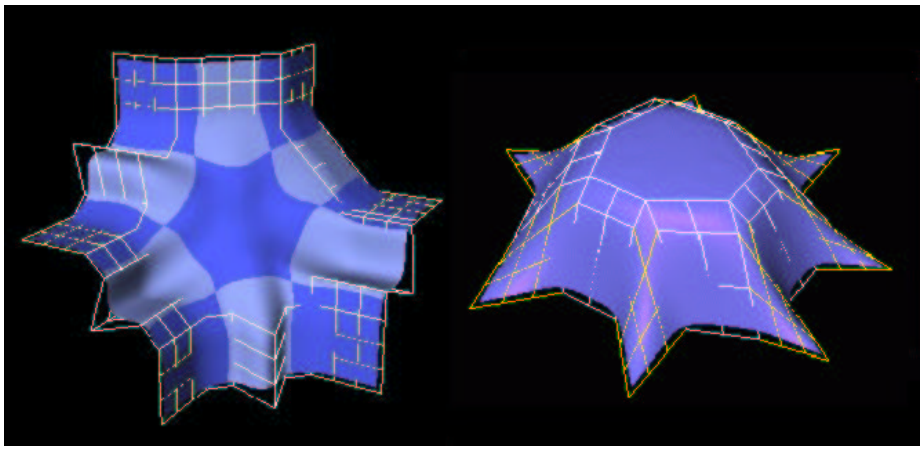

Figure 8: Two C^2 patches (6 and 7-sided) and their control meshes. Central (darker) part in the 6-sided patch corresponds to the hole in parametric space.

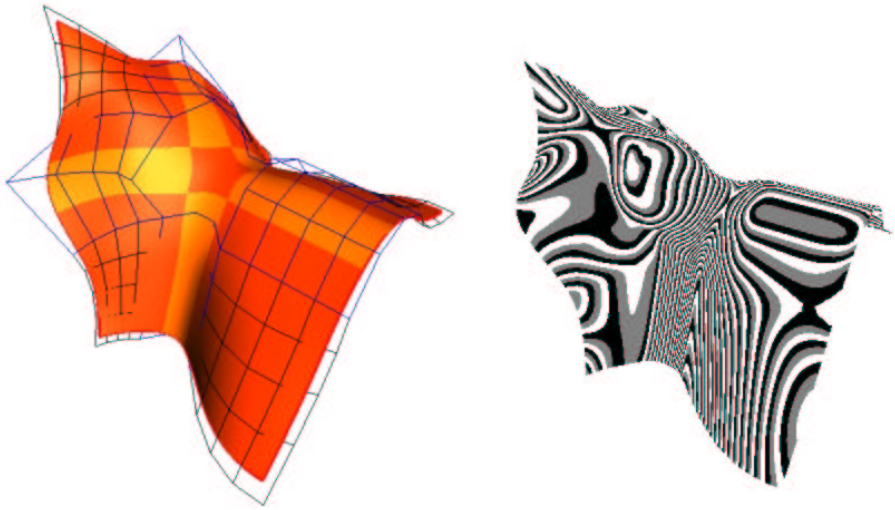

Figure 9: *Left,* a C^3 5-sided patch and its control mesh. *Right,* isophotes rendering of the same patch.

ate the shape of the resulting surface. The dark zone on the center corresponds to the hole in parametric space.

Figure 9, shows another 5-sided hole and the corresponding patch for $k = 3$. The image on the right is a representation of the isophotes to better appreciate the smoothness of the resulting surface.

The surfaces in Figure 11 are 5-sided patches for the case $k = 2$ computed using the same control mesh but using different aperture factors. The region corresponding to the central face in parametric space of the patch is colored to show the influence of the f factor. In the bottom right example, since f is too big the number of charts covering the central part is too small, and thus an almost flat zone is obtained, loosing the C^2 continuity.

An aspect that should be taken into account is that, although near each boundary of a n-sided patch the surface coincides with a B-spline, the knot sequences are not general. In fact, the knot sequence in one direction is uniform and in the other it is piecewise uniform. Thus, connecting a given rectangular B-spline with a n-sided patch can become in same cases not straightforward. Given a tensor product B-spline patch with non-uniform knot distribution, under some circumstances we can still use the knots of the given surface to construct the regular part of the n-sided patch X_n^k. That is, we can define the points of X_n^k in a way that satisfies the distribution (distances) between the given knots. In this case the n-sided patch may not be regular (in terms of the given definition), but the process applied in the previous sections can also be performed without important modifications.

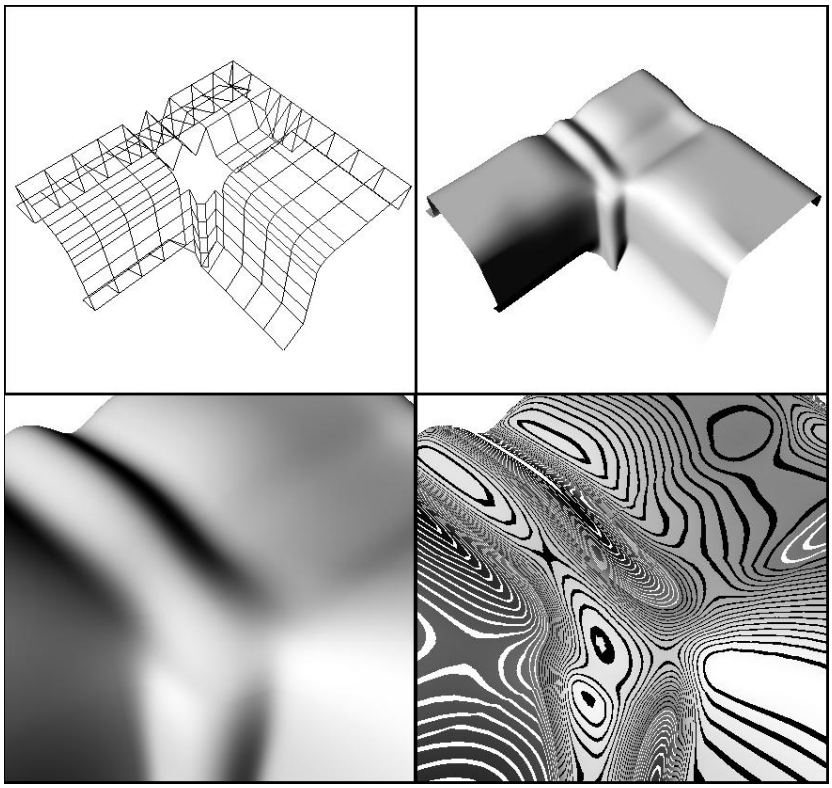

Figure 10: *Top left to bottom right:*Mesh defining a 5-sided hole, resulting patch, close-up of the central zone, and isophotes.

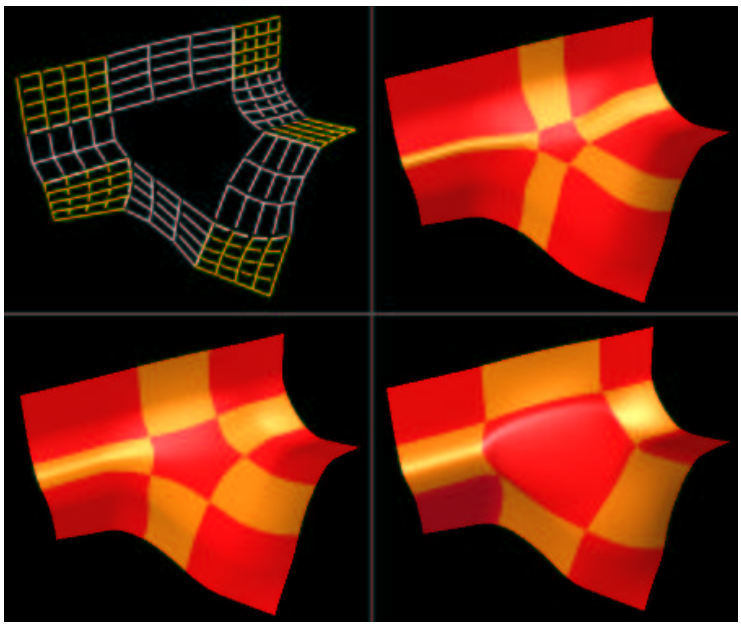

Figure 11: Three 5-sided patches defined using the same control mesh and increasing aperture factors.

8 Conclusions and future work

We have presented a method that, given a control mesh surrounding a n-sided hole constructs a patch of parametric surface of degree $k+1$ that approximates the input mesh and fills the hole. The mesh is composed of s layers of vertices distributed in n sides, and the surface near the boundaries coincides with tensor product B-spline surfaces. Since there are no restrictive conditions for neither n nor k, the proposal allows joining a given tensor product B-spline patches with GC^k.

The method only requires that the number of vertex layers s is big enough to attain the order k continuity conditions. Thus, additional layers of control points can be placed to shape the central part of the patch (without loosing the order k continuity). In addition, the method also supplies a scalar value f that can be used to have a more accurate control the influence of the control points towards the central part.

In spite of the theoretical difficulty to define the patch, we have seen that the simplicity of the construction process gives a quite easy method. We have also presented an algorithm to easily evaluate a surface point given its parametric coordinates. Furthermore, as explained the de Boor algorithm can be exploited to efficiently perform this evaluation.

The presented approach can be seen as a method that fills a n-sided hole extrapolating boundary surfaces, in a somewhat similar way than [Var91]. On

the other hand, our proposal shares with approaches [Sab83, HK84, ZA97] that it achieves a smooth connection with surrounding patches by imposing that the boundaries of the n-sided patch behave like a well known kind of surfaces.

Although our proposal allows an easy GC^k connection between an n-sided patch and a given B-spline rectangular patch, in the paper we have not treated the case of generating a patch given n rectangular patches surrounding a hole; however, we have explicited the control points and knot sequences for the B-Spline surface that coincides with our n-sided patch boundary. Future work includes analyzing the best number of additional layers of control points and its placement for usual situations in computer aided design (vertex rounding, surface bleedings, etc). Future development consists on managing the special case $n = 0$,that is, filling the hole of a ring-shaped control mesh (for example, blending the apex of a conical surface).

Another line of future work consists on choosing a different control point placement and mesh configuration for the central of the n-sided patch than the regular layer distribution one presented in this paper. Many alternative meshes and chart configurations would be supported by the generic approach of [CPV02] without loosing the B-spline boundaries property. A comparative study could be done to choose the best configuration, in terms of design flexibility and the shape of the resulting surfaces.

Appendix A

This appendix details the exact configuration of a k-continuous regular n-hole, X_n^k. Recall that we divide X_n^k into (not-disjoint) sides, notated as X_m. Besides, each side is subdivided in three submeshes, L_m, L_{m-1} and C_m. Refer to Figure 2 for a visual comprehension of the X_n^k configuration.

We label vertices of side X_0 and then, using the symmetry of the construction, labels for the other sides are defined in the same way and applying a rotation to them.

First of all we label the vertices of L_{n-1}. Bottom left vertex is labeled as l_{00}^{n-1}, and then, following a right-up order we label the rest of vertices as l_{ij}^{n-1} for $i = 0, \ldots, s$ and $j = 0, \ldots, s$. Vertices of C_0 are also labeled from left to right and from bottom to top. Bottom left vertex is c_{00}^0, and the rest of vertices are c_{ij}^0 for $i = 0, \ldots, s$ and $j = 0, \ldots, r_0$. Finally, vertices of L_0 are label in the same way, l_{00}^0 being the bottom left vertex and l_{ss}^0 the upper right one. Notice that the upper vertex row of L_{n-1} coincides with the lower row of C_0, and that the upper row of C_0 coincides with the lower row of L_0; in fact, the vertices of these two rows are those in a side that have double labelling.

To set the coordinates of vertices in X_0, we first define the angle $\alpha = 2\pi/n$, and vectors $v_0 = (1, 0)$ and $\vec{v}_1 = (\cos\alpha, \sin\alpha)$. Then, vertices $l_{ij}^0 \in L_0$, for $i = 0, \ldots, s$, $j = 0, \ldots, s$, have coordinates

$$l_{ij}^0 = i\vec{v}_0 + j\vec{v}_1 + f(sin(\alpha/2), cos(\alpha/2)) \tag{3}$$

Vertices $l_{ij}^{n-1} \in L_{n-1}$ with indices $i = 0, \ldots, s$, $j = 0, \ldots, s$ and $m = 0, \ldots, n-1$, have coordinates

$$l_{ij}^{n-1} = i\vec{v}_0 + (s-j)\vec{v}_1 + f(sin(\alpha/2), cos(\alpha/2)) \tag{4}$$

Thus, the aperture factor f is directly proportional to the size of the central face (the hole) in parametric space.

Finally, to set coordinates of the vertices in C_0 we define a polygonal curve $\mu(t) : [-1, 1] \to \mathbb{R}^2$ of minimal degree, joining the segments $\overline{l_{0s}^{-1} l_{00}^{-1}}$ and $\overline{l_{00}^{0} l_{0s}^{0}}$, with C^k continuity. This curve μ therefore fulfills:

$$\text{Endpoint interpolation:} \quad \mu(-1) = l_{0s}^{n-1} \text{ and } \mu(1) = l_{00}^{0} \tag{5}$$

$$\text{Tangency:} \quad \mu'(-1) = -\vec{v}_1 \text{ and } \mu'(1) = \vec{v}_1 \tag{6}$$

$$\forall i, 2 \leq i \leq k\,, \qquad \mu^{(i)}(-1) = \mu^{(i)}(1) = 0 \tag{7}$$

Then, vertices c_{ij}^0, for $i = 0, \ldots, s$, $j = 0, \ldots, r_0$ are defined as

$$c_{ij}^0 = \mu(t_j) + i\vec{v}_0 \tag{8}$$

with increasing parameter values $-1 = t_s < t_{s+1} < \ldots < t_{s+r_m} = 1$ such that the vertices c_{ij}^m for $j = s, \ldots, s+r_0$ are equally separated vertically. The vertical distance between points in C_m is

$$\gamma = \frac{2f}{r_m} \sin(\alpha/2) \tag{9}$$

The vertical distance between points in L_m is

$$\delta = \sin(\alpha) \tag{10}$$

As stated, vertices for the rest of sides X_m for $m = 1, \ldots, n-1$ are defined according to equations (3), (4) and (8) and applying a counterclockwise rotation of $m\alpha$ to them. In the case of vertices in C_m, the corresponding values r_m have to be substituted in the formula.

Appendix B

This appendix details the definition of the map F, which transforms a side X_0 into a rectangular shape E_0. Refer to Figure 3 for the notation used here.

The subset X_0 is the drag of a C^k curve, the left boundary of X_0, along a horizontal straight line. This C^k curve is in fact composed of three parts, the curve μ and the segments $\overline{l_{00}^{-1}, l_{0s}^{-1}}$ and $\overline{l_{00}^{0}, l_{0s}^{0}}$. Let us call $\tilde{\mu}(y)$ the horizontal distance between a point (x, y) on the left boundary of X_0 and the vertical coordinate axe $x = 0$.

Then, the C^k-continuous map F is defined as

$$\begin{array}{rccc} F & : & \mathbb{R}^2 & \to & \mathbb{R}^2 \\ & & (x, y) & \to & (x - \tilde{\mu}(y), y) \end{array}$$

Thus, F transforms the mesh X_0 into an axe-aligned rectangular mesh, E_0.

Notice that the inverse function F^{-1} maps a point (x, y) to $(x+\tilde{\mu}(y), y)$. The rest of sides E_i for $i = 1, \ldots, n-1$ can also be transformed into a rectangular lattice by applying a clockwise rotation of $i\alpha$ to them followed by the map F just being defined.

Acknowledgements

This work has been supported by the CICYT under grant TIC-99-1230-C02-02.

References

[CP00a] J. Cotrina and N. Pla. Modelling surfaces from planar irregular meshes. *Computer Aided Geometric Design*, 17:1–15, 2000.

[CP00b] J. Cotrina and N. Pla. Modelling surfaces of arbitrary topology. *Computer Aided Geometric Design*, 17:643–671, 2000.

[CPV02] J. Cotrina, N. Pla, and M. Vigo. A generic approach to free form surface generation. In *7th ACM Symposium on Solid Modelling and Applications*, pages 35–44. ACM, July 2002.

[EC97] Gershon Elber and Elaine Cohen. Filleting and rounding using trimmed tensor product surfaces. *SMA '97: Proceedings of the Fourth Symposium on Solid Modeling and Applications*, pages 206–216, May 1997. Held in held May 14-16, 1997 in Atlanta, Georgia.

[Far02] G. Farin. *Curves and Surfaces for computer aided geometric design. A Practical Guide.* Fifth Edition. Academic Press, 2002.

[HK84] M. Hosaka and F. Kimura. Non-four-sided patch expressions with control points. *Computer Aided Geometric Design*, 1(1), 1984.

[LD89] C.T. Loop and T.D. DeRose. A multisided generalization of bézier surfaces. *ACM transactions on Graphics*, 8(3):204–234, 1989.

[Mal98] P. Malraison. A bibliography for n-sided patches. In R. Crips, editor, *The Mathematics of surfaces VII, Information Geometers*, pages 419–430. 1998.

[Pra97] H. Prautzsch. Freeform splines. *Computer Aided Geometric Design*, 14:201–206, 1997.

[Sab83] M.A. Sabin. Non rectangular surface patches suitable for inclusion in B-spline surface. *Eurographics*, pages 57–69, 1983.

[SZSS98] T.W. Sederberg, J. Zheng, D. Sewell, and M. Sabin. Non uniform recursive subdivision surfaces. *Proceedings of SIGGRAPH'98*, pages 387–394, 1998.

[Var87] T. Varady. Survey and new results in n-sided patch generation. *The Mathematics of Surfaces II*, pages 203–236, 1987.

[Var91] T. Varady. Overlap patches: a new scheme for interpolating curve networks with n-sided regions. *Computer Aided Geometric Design*, 8:7–27, 1991.

[ZA97] J. Zheng and Ball A. Control point surfaces over non-four-sided areas. *Computer Aided Geometric Design*, 14:807–821, 1997.